# Collisional electron detachment and decomposition cross sections for $SF_6^-$, $SF_5^-$, and $F^-$ on $SF_6$ and rare gas targets

Yicheng Wang, R. L. Champion, and L. D. Doverspike
*Department of Physics, College of William and Mary, Williamsburg, Virginia 23185*

J. K. Olthoff and R. J. Van Brunt
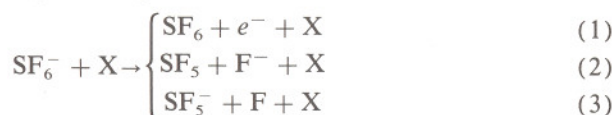*National Institute of Standards and Technology, Gaithersburg, Maryland 20899*

Absolute total cross sections for collisional electron detachment and collision-induced dissociation (CID) have been measured for binary collisions of $SF_6^-$ and $SF_5^-$ with rare gas and $SF_6$ targets for laboratory collision energies ranging from about 10 up to 500 eV. The cross sections for electron detachment of $SF_6^-$ are found to be surprisingly small, especially for the $SF_6$ target, for relative collision energies below several tens of electron volts. Specifically, detachment onsets are found to occur at around 30 and 90 eV for the rare gas and $SF_6$ targets, respectively. The CID channel which leads to $F^-$ as a product is observed to dominate detachment for relative collision energies below 100 eV. The results for the $SF_5^-$ projectile are remarkably similar to those exhibited for $SF_6^-$. The role of long-lived excited states in the reactant $SF_6$ ion beam is discussed.
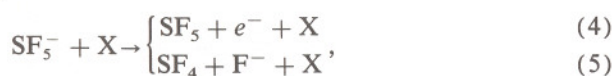
## I. INTRODUCTION

Of all complex polyatomic molecules, sulfur hexafluoride ($SF_6$) has been studied more extensively in recent years than any other.[1] This interest in $SF_6$ stems mainly from its use as a gaseous dielectric in high-voltage applications. It is attractive for such applications because of its large cross sections for direct and dissociative attachment.[2] The presence of electron detachment from anions in $SF_6$ was suspected by Schlumbohm[3] in the early 1960's. However significant uncertainties still exist concerning the identity of the ion from which the electron detaches, the magnitudes of the detachment cross sections, and the importance of detachment in discharge inception. Several discharge initiation studies indicate that cross section thresholds for collisional detachment of $SF_6^-$ may exceed the electron affinity of $SF_6$ ($\sim 1$ eV) by as much as a factor of 8.[4] Further evidence suggests that the destruction of $SF_6^-$ is dominated by collisional dissociation into various ionic fragments[5,6] rather than by the loss of an electron.

In particular, no information is available on how $SF_6^-$ decomposes in binary collisions with gaseous targets. Clearly when a complicated molecular ion such as $SF_6^-$ collides with an atom or molecule at collision energies in excess of a few electron volts, many ways of breaking up $SF_6^-$ become energetically possible. The purpose of this paper is to report the first direct measurements of various absolute cross sections for collisions of $SF_6^-$, $SF_5^-$, and $F^-$ with the rare gases and $SF_6$. The decomposition channels which are observed for $SF_6^-$ and $SF_5^-$ include

$$SF_6^- + X \rightarrow \begin{cases} SF_6 + e^- + X & (1) \\ SF_5 + F^- + X & (2) \\ SF_5^- + F + X & (3) \end{cases}$$

and

$$SF_5^- + X \rightarrow \begin{cases} SF_5 + e^- + X & (4) \\ SF_4 + F^- + X, & (5) \end{cases}$$

where X is a target atom or molecule. In addition, the detachment cross section for $F^-$ in $SF_6$ is reported and the cross sections for charge transfer of $SF_6^-$, $SF_5^-$, and $F^-$ with $X = SF_6$ have also been determined. The laboratory collision energies ($\epsilon_L$) in these experiments range from 3 up to 500 eV. Cross sections for the above channels will be denoted $\sigma_i(\epsilon_{c.m.})$ where $i = 1$ to 5 in accordance with the above reaction label numbers, and $\epsilon_{c.m.}$ is the center-of-mass energy.

## II. EXPERIMENTAL METHOD

The absolute total cross sections for the above reactions have been measured using a conventional ion-beam, gas-target technique which has been described in detail.[7] The $F^-$ ions are produced in an arc-discharge ion source which uses a mixture of $CF_4$ and argon as the discharge gas. $SF_6^-$ and $SF_5^-$ are produced when $CF_4$ is replaced with $SF_6$ in the discharge source. Due to the large electron-attachment cross section of $SF_6$, the arc discharge is quenched even though the ratio of $SF_6$ to argon in the source is as low as 5%. Nevertheless, electron attachment and dissociative attachment in the vicinity of the tungsten filament yield significant amounts of $SF_6^-$ and $SF_5^-$. Currents of more than 1 nA for each of these ions are extracted from the source, and energy analysis for the ions indicates that they are formed in a region very near the filament.

The negative ion beam is accelerated and subsequently mass selected with a high resolution 90° magnet. The ion beam is then focused into the collision chamber containing a target gas. A schematic diagram of this chamber is given in Fig. 1. The laboratory energy of the primary ion beam is determined by retardation analysis and should be accurate to within $\pm 5\%$. By appropriate manipulation of the magnetic and electrostatic fields in the collison chamber, it is possible to separate and measure the absolute total cross sections for the reaction channels indicated by reactions (1) through (5).
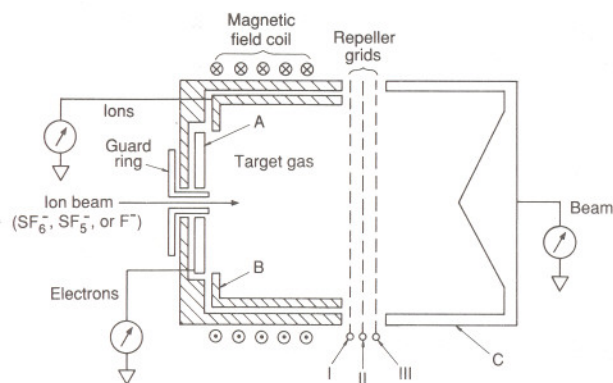
FIG. 1. Schematic of collision chamber.

The collisional-detachment cross sections $\sigma_i(\epsilon_{c.m.})$ are measured by applying a 10 G magnetic field along the beam axis together with a parallel electrostatic field between grids I and II (see Fig. 1) which serve to trap electrons that arise from detachment processes. With this arrangement, all electrons which detach in the collision region to the left of grid I are collected on element A. The neutral products in reaction channels (1) and (4) are assumed to be $SF_6 + X$ and $SF_5 + X$, respectively, although this cannot be verified in the present experiment.

In order to discuss the measurements for channels (2), (3), and (5), it is useful to assume that the dynamics of these collision-induced-dissociation (CID) channels can be described by a two-step process, e.g.,

$$SF_6^- + X \rightarrow (SF_6^-)^* + X \rightarrow \begin{cases} SF_5 + F^- + X \\ SF_5^- + F + X \end{cases},$$
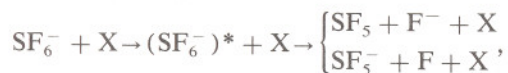
where the asterisk implies that $(SF_6^-)^*$ has been collisionally excited and contains sufficient internal energy to make dissociation energetically possible. With this assumption the different products of CID would then have roughly the same velocity but quite different kinetic energies in the laboratory reference frame, thus allowing separation of the reaction products from the different dissociation channels. For example, if the laboratory energy of the projectile $SF_6^-$ is $\epsilon_L$ (eV), then the laboratory kinetic energy for $F^-$ resulting from CID will be roughly $0.13 \epsilon_L$ and for $SF_5^-$ about $0.87\epsilon_L$. Consequently, if the voltage difference between grids I and II is, for example, $0.26\epsilon_L$ (V), then all the $F^-$ ions from CID will be reflected by the electric field between the grids and collected on elements A and B while all the $SF_5^-$ ions will be transmitted. The results of a "retardation analysis" are shown in Fig. 2 for the example of $SF_6^- +$ argon. The observation of two distinct plateau regions clearly indicates the complete separation of the $F^-$ and $SF_5^-$ ions. Thus, the CID cross sections for channels (2) and (3) may be determined using this retardation process and a separate measurement of the detachment cross section. A similar technique is used to measure the cross section for the CID channel given by channel (5).

Although the two-step model for CID is somewhat simplistic, any plausible modification of this model would not result in a substantial alteration in the kinematics for this process. Based upon the assumption that channels (2) and (3) are the sole products of CID, then the measurements for reactions (2) and (3) should be accurate to within $\pm 15\%$ and $\pm 30\%$, respectively. The larger error for reaction (3) is due to the much more limited range of retarding voltages that can be used to separate $SF_5^-$ product ions from large angle elastic or inelastic scattering of the primary ion beam. In fact, the measurements for reaction (3) are limited to projectile energies $\epsilon_L > 100$ eV.

Those products which arise from the decomposition of collisionally excited, long-lived states of $(SF_6^-)^*$ will escape detection if the $(SF_6^-)^*$ lifetime exceeds an approximate mean flight time, $\tau_f > 15/[\epsilon_L (eV)]^{1/2} \mu s$. Lifetimes on the order of 1 $\mu s$ and longer have indeed been reported[8] for $(SF_6^-)^*$, thus it is important to note that all measurements for cross sections reported herein are for "prompt" decomposition and detachment, i.e., for systems which decay in times $\tau < \tau_f$.

Special difficulties are encountered in measuring electron-detachment cross sections when $SF_6$ is used as the target gas. The number of electrons produced by interaction of the primary ion beam with the trapping and retardation grids is observed to be proportional to the intensity of the primary ion beam. Normally this signal is monitored with no target gas in the collision chamber, and routinely treated as a background signal. Accordingly this background is subtracted from the signal on element A observed when target gas is admitted to the collision chamber. Interestingly, this background signal from the grids decreases significantly when even a small amount of $SF_6$ is introduced into the collision chamber. This decrease in grid-generated background signal reaches saturation when the $SF_6$ pressure in the collision chamber is increased to $10^{-5}$ Torr. The alteration of the background signal is presumably due to $SF_6$ being adsorbed on the surfaces of the grids. Consequently, cross sections for the $SF_6$ target must be determined by using differential pressures of $SF_6$. Pressure studies (for all systems) have been
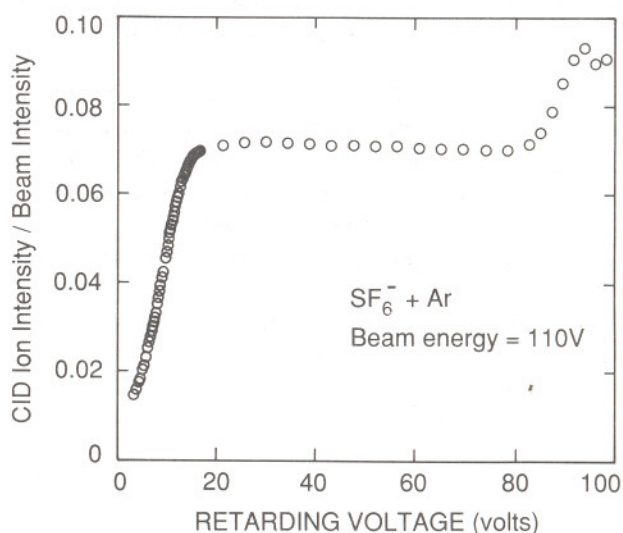


FIG. 2. Retardation analysis of CID ions for $SF_6^-$ projectiles on an argon target.

performed to insure that the measured cross sections are indeed pressure independent and that reattachment of detached electrons to the $SF_6$ target gas is insignificant.

A second difficulty which occurs with the $SF_6$ target is that charge-transfer (CT) and possibly dissociative charge-transfer (DCT) cross sections are no longer negligible. The ionic products of these reactions move slowly in the lab frame and are trapped within the electromagnetostatic trap designed to direct the detached electrons to element A. A small fraction of these slow product ions will reach element A (about 5% for an isotropic distribution of the product ions). The intensity of these ions may be determined approximately by comparing the signal observed on element A with the axial magnetic field on to that observed with the field turned off, since this field confines electrons, but has only negligible effect on ion trajectories.

## III. RESULTS

An energy level diagram for $SF_6^-$ and $SF_5^-$ and their relevant products is given in Fig. 3 for all species in their ground states.[9,10] There has been considerable uncertainty associated with the energetics of $SF_6$ and its anions, and therefore the results presented in Fig. 3 may be in need for further verification.

In the following, we will first examine the experimental results for the rare gas targets followed by those for the $SF_6$ target.

### A. Rare gas targets

The measured electron-detachment cross sections $\sigma_1(\epsilon_{c.m.})$ for collisions of $SF_6^-$ with He, Ne, Ar, Kr, and Xe are presented in Fig. 4 as a function of the relative collision energies $\epsilon_{c.m.}$. For $\epsilon_{c.m.} \leqslant 1.1$ eV (the electron affinity of $SF_6$), detachment is energetically forbidden if $SF_6^-$ is in the ground vibrational–rotational state. It is apparent from Fig. 4, however, that $\sigma_1(\epsilon_{c.m.})$ is about 1 $\text{Å}^2$ at $\epsilon_{c.m.} = 0.2$ eV for the He target, and the other rare gas targets exhibit similar behavior for energies below the electron affinity of $SF_6$. These nonzero cross sections for $\epsilon_{c.m.} \leqslant 1.1$ eV indicate that a



FIG. 4. Collisional electron-detachment cross sections for $SF_6^-$ on rare gas targets.

fraction of the $SF_6^-$ primary ion beam consists of ions produced in long-lived excited states that more readily detach upon collision. It was possible to change the fraction by altering the conditions within the ion source, namely by changing the filament temperature and gas pressure. To verify the role of excited states in the primary ion beam, experiments with the He target were performed with increased source pressure and a decreased filament temperature with consequent reduction in the fraction of excited $SF_6^-$ in the beam. As may be seen in Fig. 5, the "low-temperature"
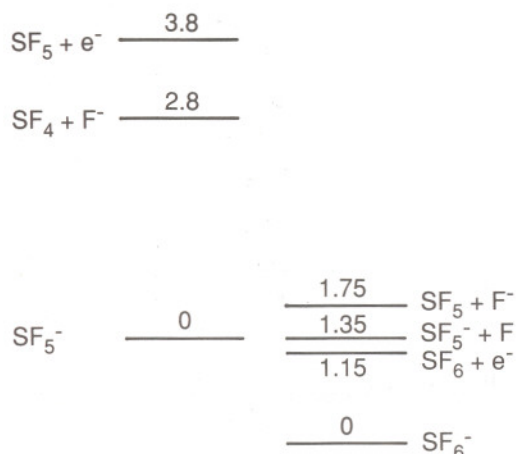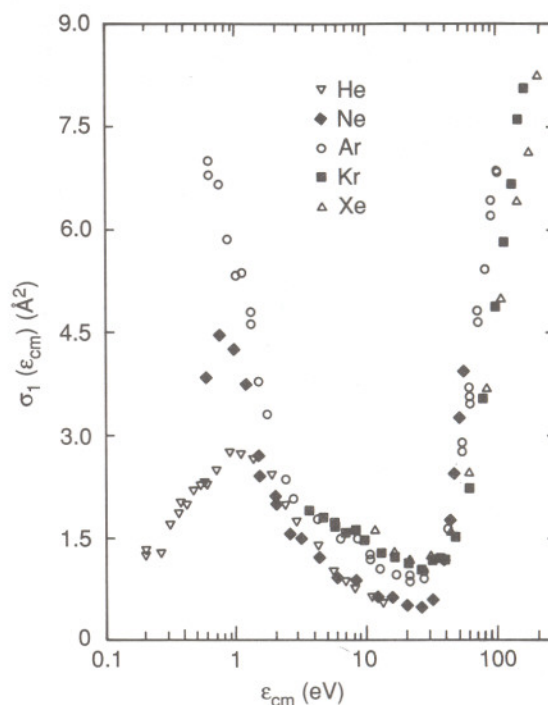


FIG. 3. Potential energy diagram for ground state $SF_5^-$ and $SF_6^-$ and their products. Values are in electron volts and are obtained from Refs. 9 and 10.
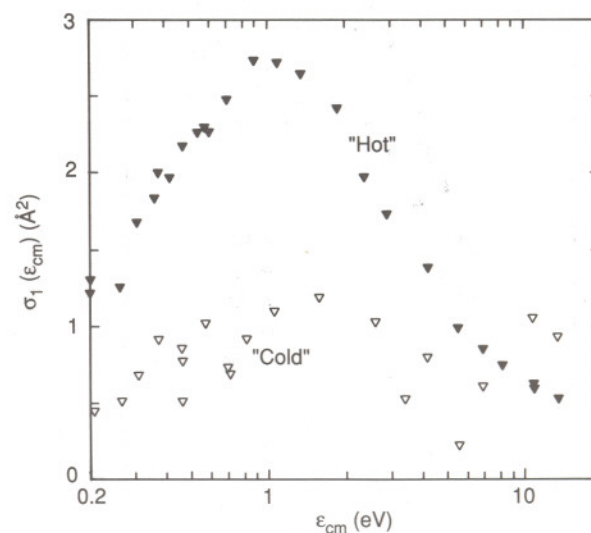


FIG. 5. Comparison of collisional electron-detachment cross sections of $SF_6^-$ on He for "hot" (solid triangles) and "cold" (open triangles) ion-source conditions.

source conditions indeed lead to a very different behavior of $\sigma_1(\epsilon_{c.m.})$ for $\epsilon_{c.m.} < 10$ eV. Even though the statistics for this latter experiment are poor (due to a substantial decrease in primary beam intensity caused by the altered source conditions), the role of excited $SF_6^-$ primary ions is obvious.

These observations are consistent with several other experimental studies which found that, under source conditions similar to those used in the present experiment, excited $SF_6^-$ ions are produced with autodetachment lifetimes which range from a few microseconds to milliseconds.[8] In fact, the evidence suggests that there exists a quasicontinuum of excited autodetaching states. Thus it is reasonable to expect that a fraction of the $SF_6^-$ beam is produced in excited states below the autodetachment threshold.

The detachment cross sections at higher collision energies exhibit rather abrupt onsets at about $\epsilon_{c.m.} = 30$ eV for all rare gas targets. For $\epsilon_{c.m.} > 30$ eV, $\sigma_1(\epsilon_{c.m.})$ is found to be relatively independent of the conditions within the ion source, suggesting that the detachment for $\epsilon_{c.m.} > 30$ eV is predominantly from energetically stable $SF_6^-$ and not significantly influenced by the initial excitation of the $SF_6^-$ projectiles.

The cross sections $\sigma_2(\epsilon_{c.m.})$ for the CID channel which produces the product $F^-$ from $SF_6^-$ projectiles are presented in Fig. 6. With the exception of He, these cross sections appear to converge to an onset near $\epsilon_{c.m.} = 2$ eV, which is close to the energetic threshold of 1.75 eV given in Fig. 3. The cross section for the He target has been measured for collision energies as low as 0.4 eV and is observed to be nonzero [i.e., $0 < \sigma_2(0.4 \text{ eV}) < 0.1 \text{ Å}^2$] for some ion source conditions which again suggests contributions from excited states of $SF_6^-$ in the primary ion beam.

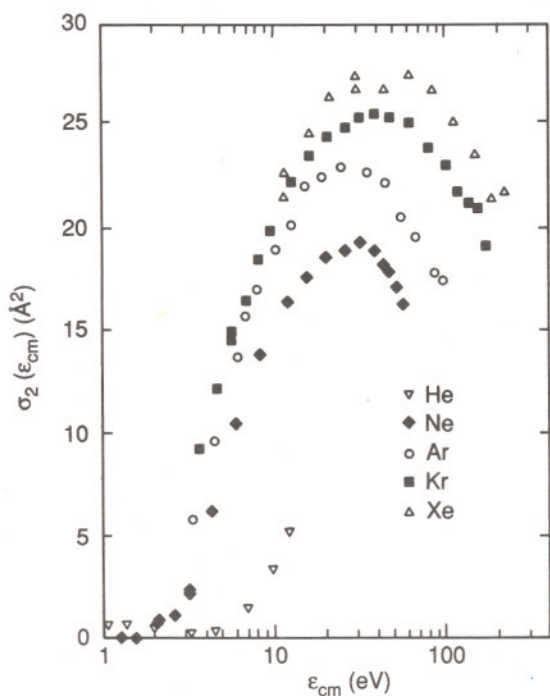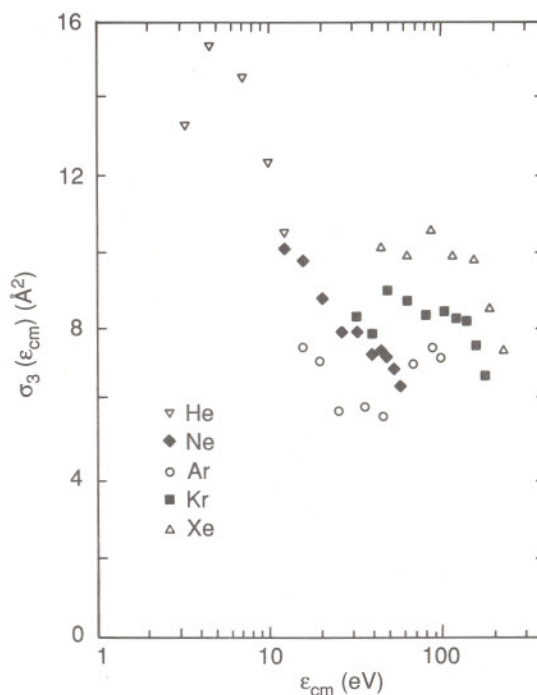The magnitude of the cross sections at the maxima ob-



FIG. 7. Measured cross sections for CID production of $SF_5^-$ from $SF_6^-$ on rare gas targets.

served in $\sigma_2(\epsilon_{c.m.})$ increases as the mass of the rare gas target increases. It can be seen that the cross section for this CID channel is considerably larger than the detachment cross section for energies in the range $10 \leqslant \epsilon_{c.m.} \leqslant 100$ eV. Additionally, it is of significance to note that the maxima in $\sigma_2(\epsilon_{c.m.})$ occur at energies near the onsets for $\sigma_1(\epsilon_{c.m.})$.

The cross sections for the CID channel $\sigma_3(\epsilon_{c.m.})$, which yields $SF_5^-$ as a product, are presented in Fig. 7.



FIG. 6. Measured cross sections for CID production of $F^-$ from $SF_6^-$ on rare gas targets.
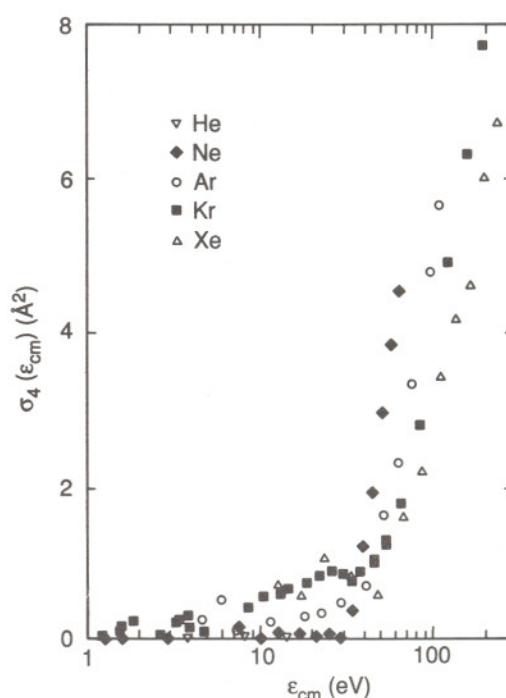


FIG. 8. Measured collisional electron-detachment cross sections for $SF_5^-$ on rare gas targets.

The electron-detachment cross sections for $SF_5^-$ on the rare gases, $\sigma_4(\epsilon_{c.m.})$, are shown in Fig. 8. For the He target, $\sigma_4(\epsilon_{c.m.})$ remains zero (i.e., $< 0.03$ Å$^2$) over the entire energy range studied for all ion source conditions. Thus, in the case of helium, there is no indication that excited states of $SF_5^-$ in the primary ion beam contribute to the detachment process. This feature of $SF_5^-$ is very different from that observed for $SF_6^-$. On the other hand, the onsets for detachment, observed at $\epsilon_{c.m.} = 30$ eV, are remarkably similar to those observed in the detachment of $SF_6^-$. This may seem somewhat surprising since the electron affinity of $SF_5$ considerably exceeds that of $SF_6$ (see Fig. 3). Below 30 eV, the cross sections are nonzero down to $\epsilon_{c.m.} < 10$ eV, with magnitudes that increase with target mass.

The results for the CID channel $\sigma_5(\epsilon_{c.m.})$, which produces $F^-$ from $SF_5^-$ projectile ions, are given in Fig. 9. The cross sections again exhibit an onset in the vicinity of the thermodynamic threshold (which appears to exceed 2 eV, see Ref. 9, 10, and 11) and are much larger than the detachment cross sections over the entire energy range of the experiments. In fact, for the He target, $\sigma_5(15 \text{ eV})/\sigma_4(15 \text{ eV}) > 200$, a result similar to that reported for reactants which involve $UF_6^-$ and the rare gases.[12]

Comparison of results shown in Figs. 9 and 6 reveal that the $\sigma_5(\epsilon_{c.m.})$ is very similar to $\sigma_2(\epsilon_{c.m.})$; in fact, the similarity in the results is such that one is tempted to conclude that these latter experiments with "$SF_5^-$" have been mistakenly performed with a primary ion beam of $SF_6^-$. This is, however, not the case.

## B. SF$_6$ target

The cross sections for detachment, $\sigma_1(\epsilon_{c.m.})$, and CID, $\sigma_2(\epsilon_{c.m.})$ and $\sigma_3(\epsilon_{c.m.})$, of $SF_6^-$ are given in Fig. 10 for an



FIG. 10. Measured cross sections for collisional detachment (▼), CID production of $F^-$ (□), CID production of $SF_5^-$ (○), and charge transfer processes (△) for $SF_6^-$ on $SF_6$ target gas. Note that the collisional-detachment data (▼) shown in the figure are multiplied by a factor of 3.

$SF_6$ target gas along with the cross sections for charge transfer which may include contributions from dissociative charge transfer. The most striking feature of the data is that $\sigma_1(\epsilon_{c.m.})$ remains remarkably small for collision energies as
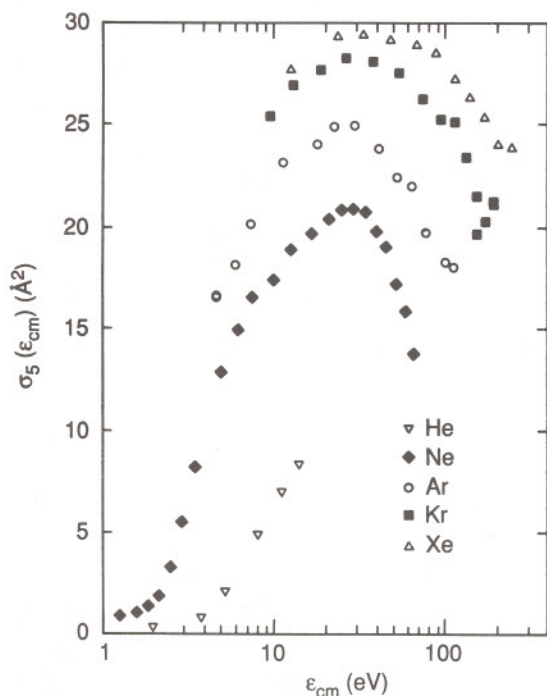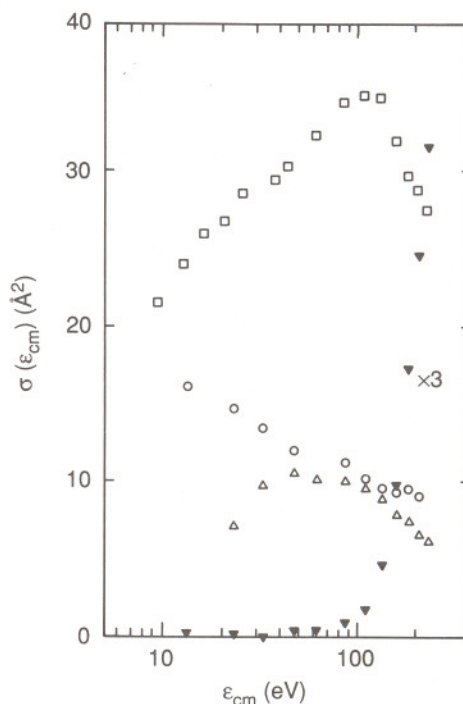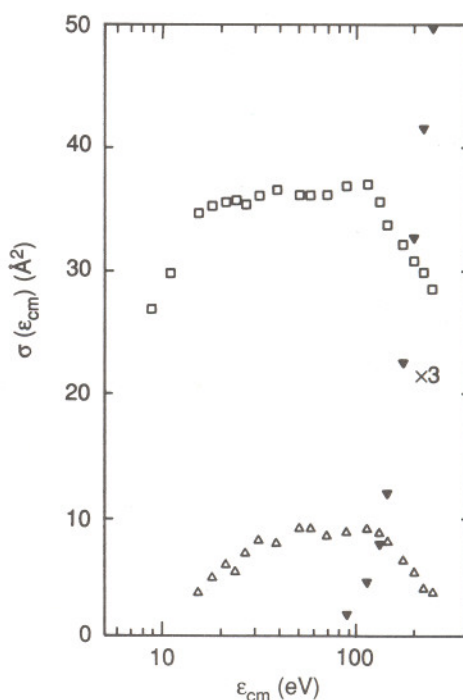


FIG. 9. Measured cross sections for CID production of $F^-$ from $SF_5^-$ on rare gas targets.



FIG. 11. Measured cross sections for collisional detachment of $SF_5^-$ (▼), CID production of $F^-$ (□), and charge-transfer processes for $SF_5^-$ (△) on $SF_6$ target gas. Note that the collisional-detachment data (▼) shown in the figure are multiplied by a factor of 3.

high as 100 eV. The experimental method and statistics are such that an upper limit on $\sigma_1(\epsilon_{c.m.})$ can be established for $\epsilon_{c.m.} \leqslant 60$ eV of $\sigma_1(\epsilon_{c.m.}) < 0.1$ Å$^2$. We are not able to extend the measurements to sufficiently low energies to ascertain whether excited states of $SF_6^-$ contribute to $\sigma_1(\epsilon_{c.m.})$ as is apparently the case for the rare gas targets. However, for $\epsilon_{c.m.} < 30$ eV, $\sigma_1(\epsilon_{c.m.})$ is significantly smaller for an $SF_6$ target than for a rare gas target of comparable mass (i.e., xenon).

The CID channel $\sigma_2(\epsilon_{c.m.})$ is again the dominant decomposition channel observed for $SF_6^-$ at energies below about 250 eV. It is likely that this trend continues for $\epsilon_{c.m.} < 10$ eV, and if so, has important implications for the modeling of discharges in $SF_6$ which will be discussed in the subsequent companion paper.[13] The cross sections for charge transfer and production of $SF_5^-$ are relatively flat, each being about 30% of $\sigma_2(\epsilon_{c.m.})$.

The results for the $SF_5^-$ projectiles are presented in Fig. 11. The various cross sections for $SF_5^-$ mimic those observed for $SF_6^-$ and the upper limit for $\sigma_4(\epsilon_{c.m.})$ below the abrupt onset at $\epsilon_{c.m.} = 90$ eV is the same as that quoted above for $\sigma_1(\epsilon_{c.m.})$.

Results for collisional-detachment and charge-transfer processes for $F^-$ on $SF_6$ are shown in Fig. 12. The detachment cross sections for $F^- + SF_6$ are very similar to those reported previously for collisions of $F^-$ with the rare gases.[14]

## IV. SUMMARY

The absolute total cross sections for prompt electron detachment and collision-induced dissociation have been measured for binary collisions of $SF_6^-$ and $SF_5^-$ with rare gas and $SF_6$ targets for laboratory collision energies below 500 eV. The salient features of these measurements are as follows. First, the cross sections for electron detachment are found to remain surprisingly small, especially for the $SF_6$ target, until collision energies in excess of tens of electron volts are reached. This observation is clearly important for the development of an understanding of electrical breakdown when using $SF_6$ as a gaseous dielectric; this will be discussed in further detail in the companion article which follows this report.[13]

It is also found that excited states of $SF_6^-$ in the primary ion beam play an important—perhaps dominant—role in electron detachment for collision energies in the vicinity of the electron affinity of $SF_6$. That excitation is undoubtedly due to the fact that a prominent way of forming $SF_6^-$ in our ion source is via electron attachment, which can yield long-lived excited states of $SF_6^-$ ions. It is only via subsequent collisions that the internal energy of the anion may be lowered; as would be the case in the present ion source as well as in other gaseous discharges. A more complete delineation of the role of excitation in the collisional decomposition of $SF_6^-$ will unfortunately be a formidable experimental challenge.

For collision energies in excess of about 30 eV, the initial internal energy of $SF_6^-$ is found *not* to influence the various decomposition cross sections. This is reasonable when the decomposition is viewed as a two-step process in which the reactant $SF_6^-$, with initial internal energy $U_1$, is collisionally excited to a higher internal energy $U_2$, which leaves the product $(SF_6^-)^*$ unstable with respect to the various decomposition channels. In reality, $U_1$ and $U_2$ may only be defined by distribution functions, but we may make some broad generalizations based upon their average values, $\langle U_1 \rangle$ and $\langle U_2 \rangle$. For large $\epsilon_{c.m.}$, $\langle U_1 \rangle / \langle U_2 \rangle$ may be small and the magnitude of $\langle U_1 \rangle$ should therefore not be important in the collisional dynamics, as is consistent with the present observations.

A reasonable extension of the two-step model discussed above would be to treat the unimolecular decomposition of the collisionally excited $SF_6^-(U_2)$ in a standard way in



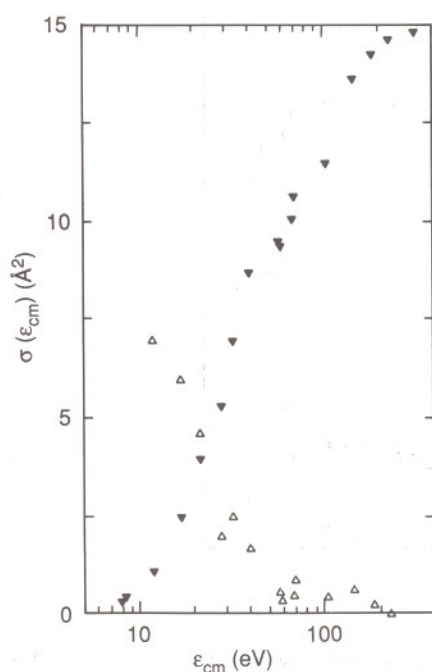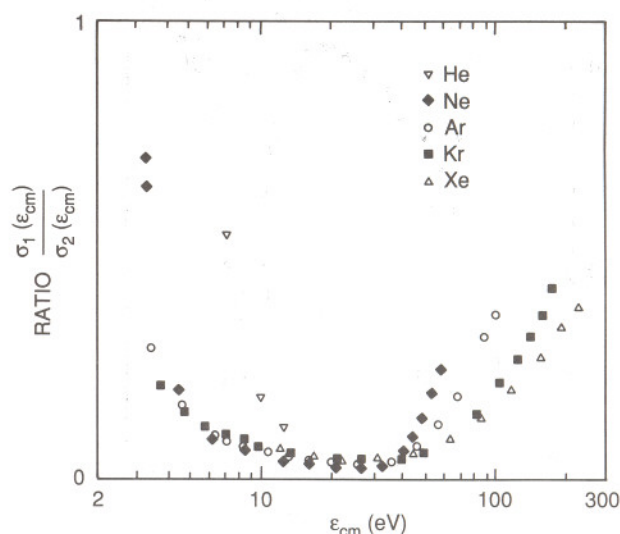FIG. 12. Measured cross sections for collisional detachment (▼) and charge-transfer reactions (△) of $F^-$ on $SF_6$ target gas.



FIG. 13. Ratio of collisional-detachment cross sections to CID cross sections for production of $F^-$:$SF_6^-$ + rare gas targets.

which the probability of decomposing into a particular product channel is taken to be proportional to the density of states for that channel.[12,15] Such a model will tend to favor the autodetachment channel when $1.15 \leqslant \langle U_2 \rangle \leqslant 1.35$ eV (see Fig. 3) but, because of phase space considerations will rapidly favor the autodissociation channels as $\langle U_2 \rangle$ is increased beyond 1.75 eV.[15] It is of interest to examine the ratio $R(\epsilon_{c.m.}) = \sigma_1(\epsilon_{c.m.})/\sigma_2(\epsilon_{c.m.})$ for the rare gas targets and this is presented in Fig. 13. The average product internal energy $\langle U_2 \rangle$ can be expected to increase as $\epsilon_{c.m.}$ increases and of course will depend upon $\langle U_1 \rangle$, which can be considered fixed for all of the data shown in Fig. 13. It can be seen that $R(\epsilon_{c.m.})$ decreases rapidly as $\epsilon_{c.m.}$ is increased beyond a few eV and remains small for all the rare gas targets for relative energies up to 30 eV. This behavior, which is seen to be quite target independent among the rare gases, is compatible with the general ideas of the model discussed above in which the intermediate excitation is followed by unimolecular decomposition. It is unreasonable to expect this model to be applied to excitation by the $SF_6$ target since a significant amount of charge transfer is observed (see Fig. 10) which is incompatible with the unimolecular-decay model. Again it should be emphasized that detachment from $SF_6^-$ is also complicated by the fact that this ion is known to have excited states of sufficiently long lifetime to preclude detection of electron release in the present experiment.

The abrupt increase in $R(\epsilon_{c.m.})$ at $\epsilon_{c.m.} > 30$ eV is due to the comparable increase in $\sigma_1(\epsilon_{c.m.})$ at 30 eV. This could be due to the onset of an additional direct detachment mechanism which is mitigated by the multidimensional equivalent of curve crossing.

An additional interesting feature of the experimental obervations is that the results for the collisonal decomposition of $SF_5^-$ (into electrons or $F^-$) are remarkably similar to those observed for $SF_6^-$. The only exception is for the collisional detachment at the lowest collision energies; $\sigma_4(\epsilon_{c.m.})$

appears to be zero below the thermodyanmic threshold (3.8 eV), implying that excited states of $SF_5^-$, if they exist, are insignificant in the reactant ion beam.

## ACKNOWLEDGMENTS

[1] See, for example, L. G. Christophorou, D. L. McCorkle, and A. A. Christodoulides, in *Electron–Molecule Interactions and Their Applications*, edited by L. G. Christophorou (Academic, New York, 1984), Vol. 1.

[2] L. E. Kline, D. K. Davies, C. L. Chen, and P. J. Chantry, J. Appl. Phys. **50**, 6789 (1979); L. G. Christophorou, D. L. McCorkle, and J. G. Carter, J. Chem. Phys. **54**, 253 (1971); A. Chutjian and S. H. Alajajian, Phys. Rev. A **31**, 2885 (1985); O. J. Orient and A. Chutjian, *ibid.* **34**, 1841 (1986).

[3] H. Schlumbohn, Z. Phys. **166**, 192 (1962).

[4] N. Wiegart, IEEE Trans. Electr. Insul. **EI-20**, 587 (1985); R. J. Van Brunt, J. Appl. Phys. **59**, 2314 (1986).

[5] B. C. O'Neill and J. D. Craggs, J. Phys. B **6**, 2634 (1973); J. de Urquijo-Carmona, I. Alvarez, and C. Cisneros, J. Phys. D **19**, L207 (1986).

[6] A. V. Phelps and R. J. Van Brunt, J. Appl. Phys. **64**, 4269 (1988).

[7] N. R. White, D. Scott, M. S. Huq, L. D. Doverspike, and R. L. Champion, J. Chem. Phys. **80**, 1108 (1984).

[8] R. W. Odom, D. L. Smith, and J. H. Futrell, J. Phys. B **8**, 1349 (1975); J. E. Delmore and L. D. Appelhans, J. Chem. Phys. **84**, 6238 (1986).

[9] E. C. M. Chen, L. Shuie, E. D. D'sa, C. F. Batten, and W. E. Wentworth, J. Chem. Phys. **88**, 4711 (1988).

[10] D. L. Hinderbrand, J. Phys. Chem. **77**, 897 (1973).

[11] The near-threshold data are broadened because of, among other things, the thermal motion of the target gas. The present results are compatible with on onset which is as high as 2.8 eV. The subject of such thermal broadening is discussed by P. J. Chantry, J. Chem. Phys. **55**, 2746 (1971).

[12] S. E. Haywood, L. D. Doverspike, R. L. Champion, E. Herbst, B. K. Annis, and S. Datz, J. Chem. Phys. **74**, 2845 (1981).

[13] J. K. Olthoff, R. J. Van Brunt, Y. Wang, R. L. Champion, and L. D. Doverspike, J. Chem. Phys. **91**, 2261 (1989).

[14] M. S. Huq, L. D. Doverspike, R. L. Champion, and V. A. Esaulov, J. Phys. B **15**, 951 (1982).

[15] C. E. Klots, J. Phys. Chem. **75**, 1526 (1971).

[16] C. E. Klots, Chem. Phys. Lett. **38**, 61 (1976).